Nov 6th, 12:00 AM - 12:00 AM

Finite Element Modeling of New Composite Floors Having Cold-Formed Steel and Concrete Slab

Yazdan Majdi

Cheng-Tzu Thomas Hsu

Mehdi Zarei

Twenty-Second International Specialty Conference on Cold-Formed Steel Structures
St. Louis, Missouri, USA, November 5 & 6, 2014

Finite Element Modeling of New Composite Floors Having Cold-Formed Steel and Concrete Slab

By Yazdan Majdi[1], Cheng-Tzu Thomas Hsu[2], and Mehdi Zarei[3]

Abstract

In this research, the structural behavior of a new type of U.S. patented composite floor system is explored through finite element modeling. The new composite floor incorporates cold-formed (light-gauge) steel profiles as the joist on bottom, a corrugated steel deck as the formwork for concrete, a hat channel (furring channel) as the continuous shear connector and finally a concrete slab on top. All steel parts in the system are cold-formed and connected together by self-drilling fasteners. In this study, a comprehensive three-dimensional finite element modeling is performed for the composite floor system. A local bond-slip model is applied to simulate the slip of the shear connector inside the concrete slab. A nonlinear analysis is performed on the composite floor considering all different types of structural nonlinearities and the behavior of the system is monitored from beginning of loading all the way to failure. Results of finite element analysis are compared with experimental results. Further, during the course of this study, several parametric studies are conducted to determine the effect of bond-slip behavior on reducing ultimate strength and initial stiffness of such a floor system.

[1] PhD, PE, Structural Engineer, Arup, New York, NY 10005.
[2] PhD, PEng, Professor and Director of High Performance Concrete Structures Laboratory, Dept. of Civil and Environmental Engineering, New Jersey Institute of Technology, Newark, NJ 07102.
[3] PhD Candidate, Department of Civil and Environmental Engineering, New Jersey Institute of Technology, Newark, NJ 07102

Introduction

The basic idea in composite construction is to use the advantages of both steel and concrete materials while avoiding their inherent disadvantages. In order for this idea to work, steel and concrete parts should be fully connected so that no delamination and/or slip can occur between the two parts when loaded. This research focuses on analytically studying a new type of composite floor system with cold-formed steel having an innovative type of shear connector. The floor system is patented in the U.S. (Hsu, et al, 2010) and is illustrated in Figure 1.

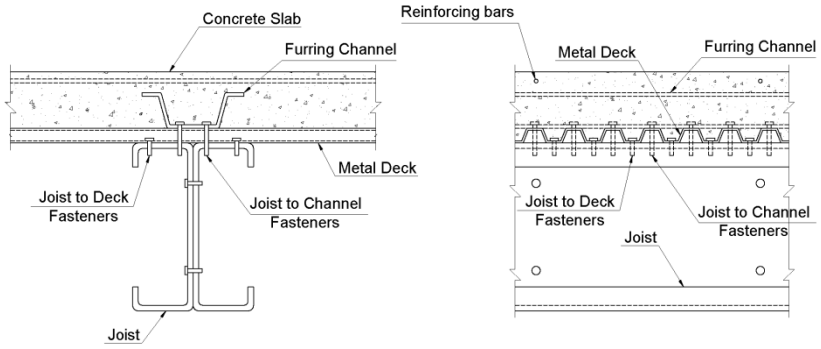

Figure 1 Configuration of the new proposed composite floor system

In this cold-formed composite floor system, a continuous furring channel has been used instead of shear studs, as the shear connector. The structural system consists of: steel joists comprising two back-to-back C-sections, a corrugated steel deck (which also acts as formwork for the concrete slab), furring channels as the shear connector and a cast-in-place concrete slab with transverse reinforcement. Self-drilling fasteners are used for connecting the steel parts of the system. The furring channel is expected to transfer shear forces from the steel joist to the slab through its bond-slip behavior. Thus, the bond-slip mechanism is the key parameter in studying the effectiveness of the furring channel.

The objective of this research is to use computer modeling (simulation) to study the structural behavior of such a composite floor system. Finite Element Method will be used for the purpose of structural modeling and analysis. Experimental results will be used to validate the performed finite element modeling. Structural behavior of the proposed composite floor system will be studied up to a defined point of failure, capability of the newly introduced shear connector to maintain composite action between steel joist and concrete will be evaluated and the

effect of its slip on behavior of the system will be studied in the finite element simulation.

General Modeling Assumptions

In finite element modeling of the floor system, a single steel joist plus an effective width of the above concrete slab and steel deck are considered based on AISC recommendations (2005, 2011). In all models, steel joist is made of two AISI standard C sections (introduced in Table 1 for each model) and steel deck is an AISI standard 9/16" cold-formed deck (gauge 20) with proof stress of 33 ksi. The continuous shear connector is a cold-formed hat channel. All models are assumed to be simply-supported in both ends and are loaded with two vertical concentrated loads (equal to P/2) in one third and two third of the span. It is assumed that self-weight of the system also appears as two equivalent concentrated loads in one third and two third of the span. This idealization causes minor error in analysis results as the effect of self-weight is insignificant.

Modeling Cold-formed Steel Material

The cold-formed steel material is assumed to follow a multi-linear stress-strain pattern in uniaxial tension. The multi-linear patterns are chosen to agree with actual stress-strain curves obtained from tension tests on material coupons. For all cold-formed steel materials, von Mises yield criterion is used with associative flow rule and isotropic (work) hardening rule (Ansys Inc, 2009a). Poisson's ratio for cold-formed steel is assumed to be equal to 0.3.

Modeling Concrete Material

A multi-linear uniaxial stress-strain relationship in compression is assumed for concrete based on the following numerical expression as suggested by Desayi and Krishnan (1964):

$$f = \frac{E_c \varepsilon}{1 + \left(\frac{\varepsilon}{\varepsilon_0}\right)^2} \quad (1)$$

$$\varepsilon_0 = \frac{2f'_c}{E_c} \quad (2)$$

Where:
f = stress at strain ε
ε = strain at stress f
ε_0 = strain at the ultimate compressive strength, f'_c
E_c = concrete modulus of elasticity (equal to initial slope of the curve), determined from the equation suggested in ACI code (2011):

$$E_c = 57000\sqrt{f'_c} \quad (3)$$

In which fc' should be in psi, or:

$$E_c = 4700\sqrt{f'_c}$$

In which f'c should be in MPa.

The softening branch of stress-strain curve of concrete is approximated by a perfectly plastic behavior beyond the point of ultimate stress to overcome convergence problems. Plasticity is considered in the concrete model using von Mises yield criterion, associative flow rule and isotropic (work) hardening (Ansys Inc, 2009a). No crushing is assumed for the concrete. When tensile principal stress in a point attains the value of fct (splitting tensile strength), concrete is assumed to crack perpendicular to the direction of stress in that point. The tensile stress in point of crack will suddenly be dropped to zero. Tensile behavior of concrete is assumed to be linear before cracking. The value of fct is assumed equal to the average splitting tensile strength suggested in the commentary of ACI code (2011) section R8.6.1:

$$f_{ct} = 6.7\sqrt{f'_c} \quad (4)$$

In which f'_c should be in psi, or:

$$f_c = 0.56\sqrt{f'_c}$$

In which f'_c should be in MPa.
Poisson's ratio for concrete is assumed equal to 0.2.

Modeling Structural Components

Concrete slab is modeled using the brick element SOLID65 in ANSYS (Ansys Inc., 2009b). The element is capable of developing smeared cracks Cold-formed steel parts are all modeled using SHELL181 element. The element is well-suited for linear, large rotation, and/or large strain nonlinear applications.
Refer to Figure 2 and Figure 3 for elements meshing and types of elements used for steel and concrete parts.

Bond-slip Behavior between Furring Channel and Concrete

In the proposed composite floor system, shear transfer between the steel joist and concrete slab relies on the bond-slip behavior between the faces of the continuous furring channel and concrete. A local bond-slip model is required to simulate such behavior in Finite Element Analysis. Local bond-slip model is referred to a graph or function which expresses bond stress (shear stress

transferred over the steel and concrete faces, τ) in terms of the slip between the contact faces (δ) at any arbitrary point of contact. Majdi (2013) developed and verified such a local bond-slip model which the model will be used in this research. In the Finite Element Models, the concrete deck is connected to the furring channel through surface-to-surface contact and target elements, CONTA173 and TARGET170 (Ansys Inc., 2009b), to simulate the bond-slip condition between the two materials (see Figure 4).

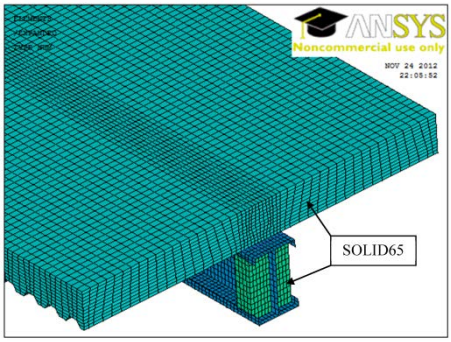

Figure 2 Elements used for modeling (1/2)

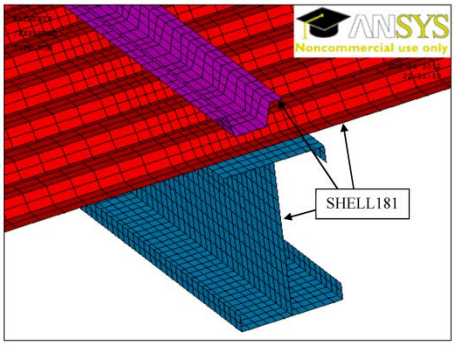

Figure 3 Elements used for modeling (1/2)

Contact between Concrete Slab and Steel Deck

The contact behavior between concrete slab and steel deck is also considered here and is modeled with the pair of CONTA173 / TARGE170 elements as described above. In this case, the two faces are constrained such that they are not able to penetrate into each other; however they are free to slip and get separated. The contact surfaces are assumed friction-free and "no-penetration" is the only constrain (see Figure 4).

Modeling Connectivity with Screws

All short screws are assumed to create a no-slip condition between the two connecting faces. The effect of bending in long screws is accounted for by using beam elements between the furring channel and the steel joist. Additionally, screws are assumed to have adequate strength to maintain connectivity between steel parts until the end of analysis.

CONTA178 element is used to model the connectivity between any two faces attached with a screw (Ansys Inc., 2009b). This connectivity is assumed to be over multiple pairs of nodes rather than one single pair of node on the contacting

faces. CONTA178 is a node-to-node contact element. The contact behavior between each node pair is assumed perfectly bonded in all directions. The average of forces transmitted between the two sides of the contact can be interpreted as forces in the screw connecting the two faces.

BEAM188 element is used to model the connectivity of long screws between furring channel and the steel joist (Ansys Inc., 2009b). Once again the connectivity is assumed to be over multiple pairs of nodes rather than one single pair of node. The average of shear forces and bending moments in all beam elements can be interpreted as the shear force and bending moment in the attaching long screw. Values of axial and flexural stiffness for the beam elements are adjusted to match the actual stiffness of the connecting screw. Refer to Figure 5 for finite element modeling of fasteners.

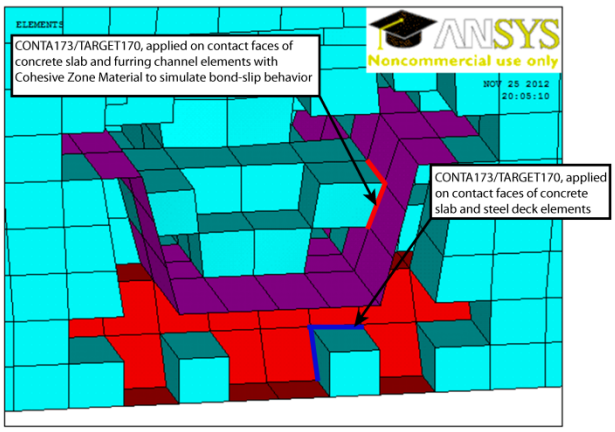

Figure 4 Furring channel surrounded by concrete elements

Furring Channel with Cut and Bent Ribs

As a modification to the regular set-up, some cuts are made on the shear connector's lips at longitudinal distances of every 1 foot (30.48 cm) to study their effect on the system's structural behavior. The cut edges are then bent up to form some ribs which will interlock into the concrete and provide better integrity. Finite element modeling of these bent ribs is shown in Figure 6. Surfaces of the ribs are in contact with the concrete having the same assumption as the one made for the whole shear connector. Additionally, a hinge connection has been considered at the bottom of ribs to account for the fact that steel has yielded in the process of bending up in those areas.

Analysis Assumptions

Nonlinear analysis is performed on each model using the Newton-Raphson method. All models are loaded gradually in many steps. The amount of loading is increased until the maximum principal compressive strain in concrete elements on the top attains the value of 0.003 which is the amount of ultimate strain for concrete proposed by the ACI code (2011). The analysis will stop then and the total amount of the applied load in the last step will be recorded as the ultimate strength (ultimate load) of the system. There will be three types of nonlinearity in the system: 1) Material nonlinearity, 2) Large deformation and 3) Contact behavior.

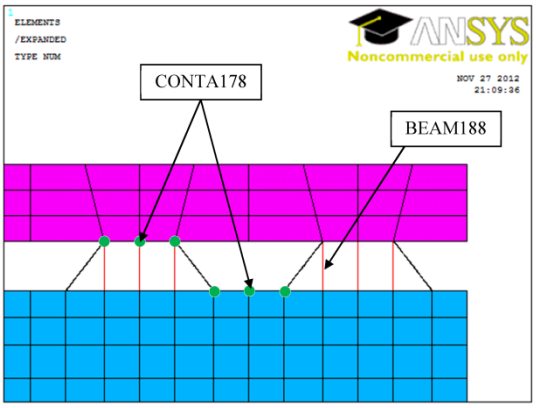

Figure 5 Modeling of screws

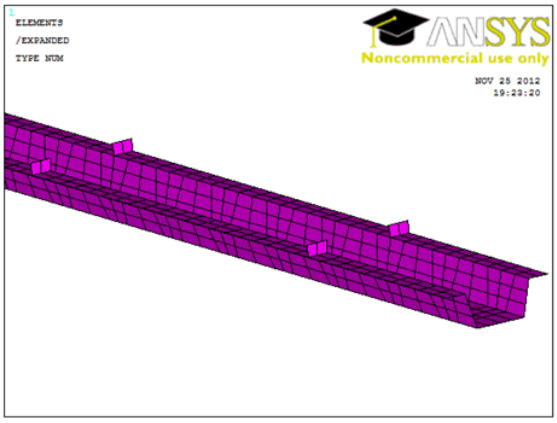

Figure 6 Modeling cut and bent ribs on the furring channel

Designation of Models

Each model is designated by a capital letter “A”, “B”, “C” followed by a number and ending with either letter “p” or “b”. The first capital letter specifies the category of the model. Models from category “A” are with regular or cut & bent ribs on the furring channel and their results will be compared with the existing experimental data by Punurai (2007). Category “B” models are created to study the effect of shear connector’s slip in concrete on the system’s behavior for different span lengths. Category “C” models are created to study the effect of shear connector’s slip in concrete on the system’s behavior for different values of section’s moment of inertia. Letter “p” in the end of a model’s name shows that the shear connector in that model is perfectly bonded with the surrounding concrete. On the other hand, letter “b” shows that the shear connector in that model has a bond-slip behavior inside the concrete following the bi-linear model proposed by Majdi (2013).

A list of all models together with their specifications is given in Table 1. Note that models B3p, B3b, C2p and C2b are repetitive to make comparisons easier. In all models, height of concrete is measured from the lower steel deck’s rib to the top of concrete and Fy represents proof stress of cold-formed steel.

Results for Category “A” Models

In Figure 7 through Figure 9, load-deformation graphs for category “A” models are illustrated and compared with experimental data.
It is observed that:
- Results of finite element modeling for the proposed composite floor system are in good agreement with the experimental data.
- The finite element analyses presented here lead to more conservative results as compared with the experiments.
- Cut and bent ribs of the shear connector do not significantly improve the ultimate strength and the general structural behavior of the system based on the present finite element modeling and the test results by Punurai (2007).
- The new proposed shear connector (the furring channel) is successfully capable of developing a composite action in the system. Figure 10 shows distribution of the bond stress on surface of the furring channel agrees with shear diagram of the composite beam which proves the shear transfer has been successfully provided by the furring channel up to the ultimate load.

Table 1 List of Finite Element Models with Their Specifications

Model Name	Steel Joist Section[1]	Concrete Slab's Height[2], in (cm)	Concrete Slab's Width, ft (m)	Span Length, ft (m)	f'_c ksi (MPa)	F_y[3] ksi (MPa)	Shear Connector Type	Bond Slip Behavior Applied?
A1p	600S200-68	3.5 (8.89)	3 (0.914)	12 (3.66)	3.2 (22.06)	41 (282.68)	Regular	NO
A1b	600S200-68	3.5 (8.89)	3 (0.914)	12 (3.66)	3.2 (22.06)	41 (282.68)	Regular	YES
A2p	600S200-68	3.5 (8.89)	3 (0.914)	12 (3.66)	3.2 (22.06)	41 (282.68)	With Cut & Bent	NO
A2b	600S200-68	3.5 (8.89)	3 (0.914)	12 (3.66)	3.2 (22.06)	41 (282.68)	With Cut & Bent	YES
A3p	600S200-54	3 (7.62)	3 (0.914)	12 (3.66)	2.3 (15.86)	37 (255.11)	With Cut & Bent	NO
A3b	600S200-54	3 (7.62)	3 (0.914)	12 (3.66)	2.3 (15.86)	37 (255.11)	With Cut & Bent	YES
B1p	600S200-68	3.5 (8.89)	3 (0.914)	8 (2.44)	3.2 (22.06)	41 (282.68)	Regular	NO
B1b	600S200-68	3.5 (8.89)	3 (0.914)	8 (2.44)	3.2 (22.06)	41 (282.68)	Regular	YES
B2p	600S200-68	3.5 (8.89)	3 (0.914)	10 (3.05)	3.2 (22.06)	41 (282.68)	Regular	NO
B2b	600S200-68	3.5 (8.89)	3 (0.914)	10 (3.05)	3.2 (22.06)	41 (282.68)	Regular	YES
B3p	600S200-68	3.5 (8.89)	3 (0.914)	12 (3.66)	3.2 (22.06)	41 (282.68)	Regular	NO
B3b	600S200-68	3.5 (8.89)	3 (0.914)	12 (3.66)	3.2 (22.06)	41 (282.68)	Regular	YES
B4p	600S200-68	3.5 (8.89)	3 (0.914)	16 (4.88)	3.2 (22.06)	41 (282.68)	Regular	NO
B4b	600S200-68	3.5 (8.89)	3 (0.914)	16	3.2 (22.06)	41 (282.68)	Regular	YES
C1p	600S200-97	3.5 (8.89)	3 (0.914)	12 (3.66)	3.2 (22.06)	41 (282.68)	Regular	NO
C1b	600S200-97	3.5 (8.89)	3 (0.914)	12 (3.66)	3.2 (22.06)	41 (282.68)	Regular	YES
C2p	600S200-68	3.5 (8.89)	3 (0.914)	12 (3.66)	3.2 (22.06)	41 (282.68)	Regular	NO
C2b	600S200-68	3.5 (8.89)	3 (0.914)	12 (3.66)	3.2 (22.06)	41 (282.68)	Regular	YES
C3p	600S200-68	3 (7.62)	3 (0.914)	12 (3.66)	3.2 (22.06)	41 (282.68)	Regular	NO
C3b	600S200-68	3 (7.62)	3 (0.914)	12 (3.66)	3.2 (22.06)	41 (282.68)	Regular	YES
C4p	600S200-54	3 (7.62)	3 (0.914)	12 (3.66)	3.2 (22.06)	41 (282.68)	Regular	NO
C4b	600S200-54	3 (7.62)	3 (0.914)	12 (3.66)	3.2 (22.06)	41 (282.68)	Regular	YES

1. Designation as adopted by AISI Standard (2002), e.g., 600S200-68 means cold-formed C section with total height of 6 inches, flange width of 2 inches and nominal thickness of 0.068 inch (for SI, 1 inch = 2.54 cm).
2. Measure from top of steel deck's rib.
3. Proof stress of cold-formed steel, obtained from 0.2% offset method.

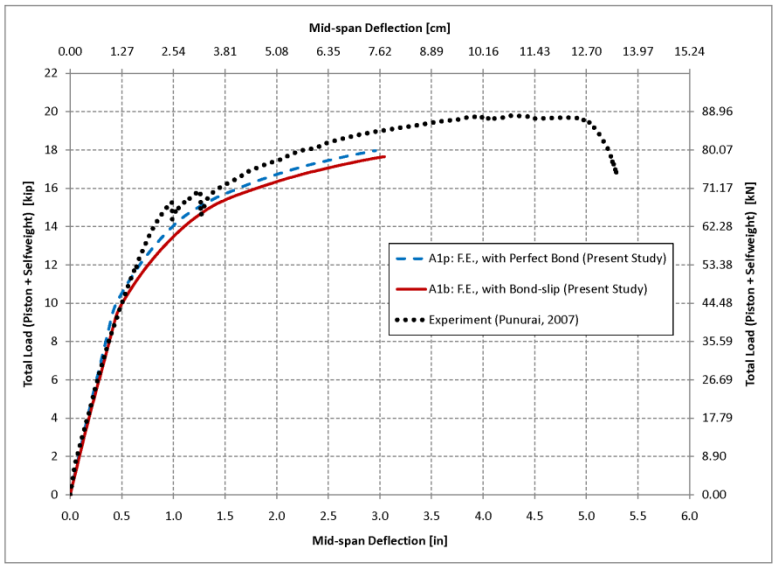

Figure 7 Comparison of load-deformation between FEM and experiment (1/3)

Table 2 Comparison of Ultimate Total Loads for Different Values of Moment of Inertia over Span Lengths

Model	M.I. / Span, in^3 (cm^3)	Ultimate Total Load, kips (kN)		% Reduction due to Bond-slip
		Perfect Bond Condition	Bond-slip Applied	
B1p & B1b	0.5450 (8.9309)	26.455 (117.68)	22.961 (102.14)	13.207
B2p & B2b	0.4360 (7.1448)	19.643 (87.38)	18.836 (83.79)	4.108
B3p & B3b	0.3634 (5.9551)	17.964 (79.91)	17.644 (78.48)	1.781
B4p & B4b	0.2725 (4.4655)	13.264 (59.00)	13.223 (58.82)	0.309
C1p & C1b	0.4672 (7.6560)	23.043 (102.50)	21.412 (95.25)	7.078
C2p & C2b	0.3634 (5.9551)	17.964 (79.91)	17.644 (78.48)	1.781
C3p & C3b	0.3073 (5.0357)	15.429 (68.63)	15.31 (68.10)	0.771
C4p & C4b	0.2587(4.2393)	12.911 (57.43)	12.88 (57.29)	0.240

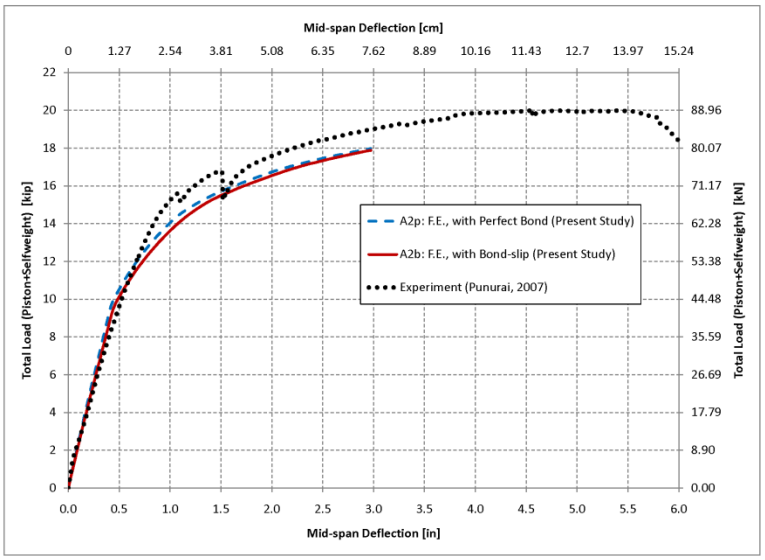

Figure 8 Comparison of load-deformation between FEM and experiment (1/3)

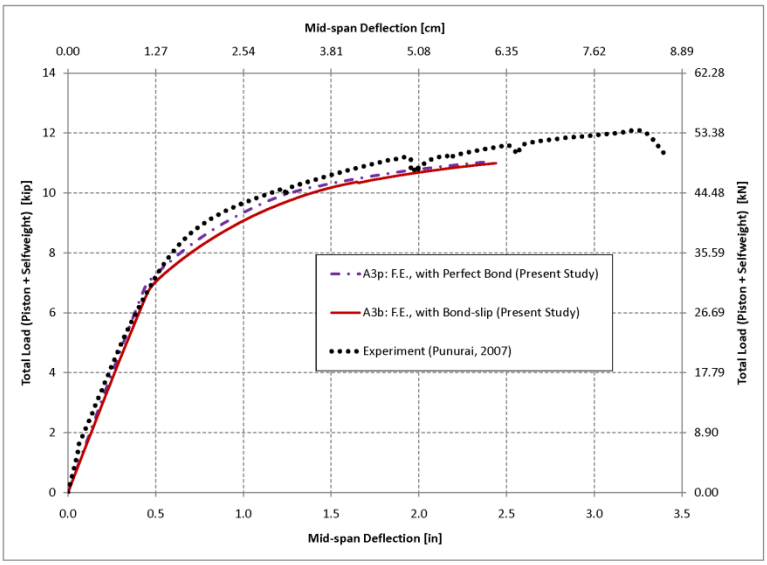

Figure 9 Comparison of load-deformation between FEM and experiment (1/3)

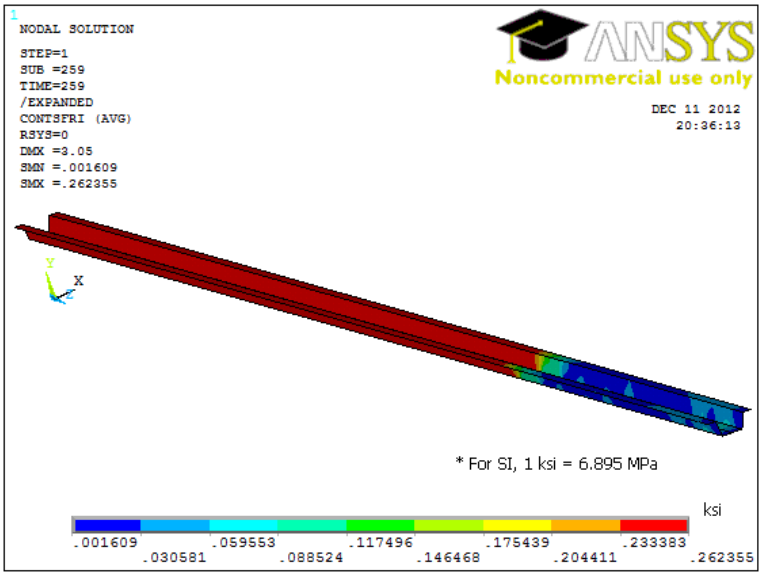

Figure 10 Distribution of bond stress at ultimate load in model A2b

Results for Category "B" and "C" Models

Load-deformation graphs for category "B" models are shown in Figure 11. It is observed that as the span length increases, the effect of bond-slip on structural response of the system reduces. All category "C" models have the same span lengths of 12 feet (3.66 m) and the same material properties and concrete slab width. However, different values of section's moments of inertia are used in the finite element modeling by changing the joist thickness and the height of concrete slab. The load-deformation graphs for these models are shown in Figure 12. It is observed that as the section's moment of inertia decreases, the effect of bond-slip on structural response of the system reduces. The moment of inertia calculated for category "C" models are based on non-slip condition and no crack in concrete.

It is concluded that for each one of models in category "B" and "C", the value of moment of inertia over span length can be chosen as a parameter to represent the effectiveness of bond-slip behavior in structural response of the system.
Values of ultimate loads and initial slopes of load-deformation graphs (initial stiffness) are compared versus moment of inertia over span lengths as depicted in Table 2 and Table 3, respectively.

In order to quantify the effect of bond-slip behavior on ultimate load and stiffness of the proposed composite floor system, the following equations are suggested by curve fitting through all cases studied:

$$PRU = 394.16\ (\frac{I}{L})^{5.42} \quad (10)$$

$$PRS = 27.78\ (\frac{I}{L}) \quad (11)$$

Where:
PRU = Percentage reduction in ultimate load due to bond-slip behavior [%]
PRS = Percentage reduction in stiffness (initial slope of load-deformation graph) due to bond-slip behavior [%]
I = Moment of inertia of the composite section [in4] (concrete is converted to an equivalent steel, with no cracking in concrete and no slip between steel and concrete).
L = Span length of the composite beam [in].
In SI units, the equations will take the following form:

$$PRU = 0.000104\ (\frac{I}{L})^{5.42}$$

$$PRS = 1.691\ (\frac{I}{L})$$

Where $\frac{I}{L}$ has unit of cm^3.

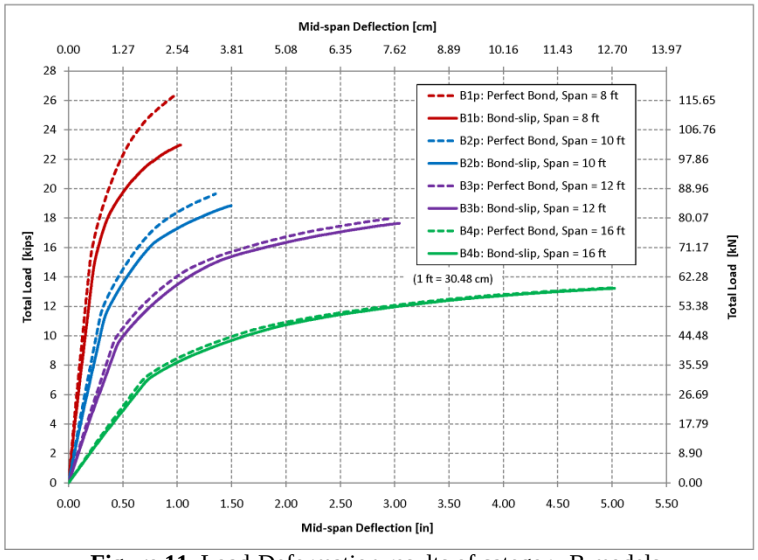

Figure 11 Load-Deformation results of category B models

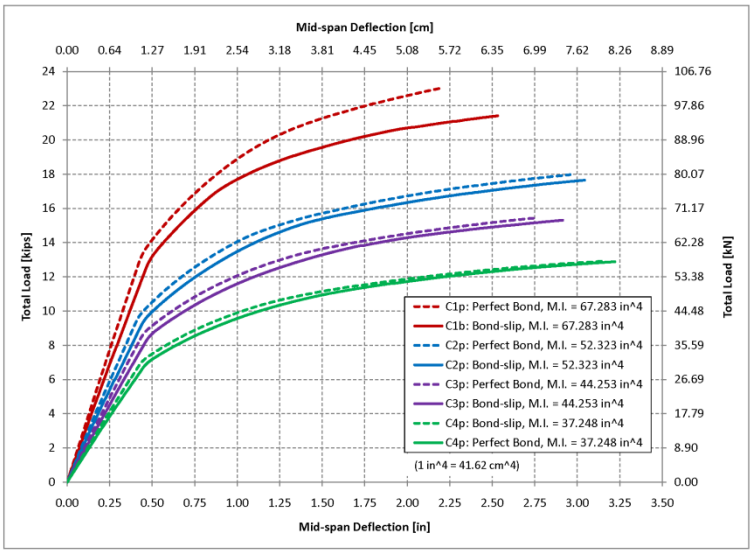

Figure 12 Load-Deformation results of category C models

Table 3 Comparison of Initial Slopes of Load-deformation Graphs (Stiffness) for Different Values of Moment of Inertia over Span Lengths

Model	M.I. / Span, in^3 (cm^3)	Initial Slope of the Graph, kips/in (kN/cm)		% Reduction due to Bond-slip
		Perfect Bond Condition	Bond-slip Applied	
B1p & B1b	0.5450 (8.9309)	74.282(130.088)	62.791(109.964)	15.469
B2p & B2b	0.4360 (7.1448)	38.5 (67.424)	33.875 (59.324)	12.013
B3p & B3b	0.3634 (5.9551)	23.041 (40.351)	20.774 (36.381)	9.839
B4p & B4b	0.2725 (4.4655)	10.358 (18.140)	9.555 (16.733)	7.752
C1p & C1b	0.4672 (7.6560)	30.518 (53.445)	26.667 (46.701)	12.619
C2p & C2b	0.3634 (5.9551)	23.041 (40.351)	20.774 (36.381)	9.839
C3p & C3b	0.3073 (5.0357)	19.445 (34.053)	17.776 (31.131)	8.583
C4p & C4b	0.2587(4.2393)	16.142 (28.269)	14.943 (26.169)	7.428

Conclusions

It is concluded from the present finite element modeling that using a multi-linear material nonlinearity combined with large-deformation geometrical nonlinearity yields reasonable results which are in good agreement with the experimental data. In this study, the finite element analysis by ANSYS terminates in computation as soon as the compressive principal strain on the top of the concrete reaches the value of 0.003 as suggested in the ACI code (2011) and the corresponding load is considered as the ultimate total load on the system. It is found that the proposed furring channel profile as the shear connector is able to effectively provide the necessary shear transfer mechanism between steel and concrete for both before and after the application of bond-slip behavior to the composite floor system. Applying the bond-slip behavior between steel and concrete to the composite floor system will decrease the ultimate strength and the initial stiffness of the system in comparison with a perfect bond condition. This decrease is more significant for systems with higher values of moment of inertia over span length. Empirical equations are derived and suggested in this study to determine the percentage decrease in the ultimate strength and stiffness of the system.

Appendix-References

ACI Committee 318. (2011). Building Code Requirements for Structural Concrete (ACI 318-05) and commentary (ACI 318R-05). Michigan.

AISC. (2005, 2011). Specification for Structural Steel Buildings. Chicago, Illinois: American Institue of Steel Construction.

AISI. (2002). Cold-formed Steel Design. Washington, DC: American Iron and Steel Institute.

Ansys Inc. (2009a). Theory Reference for the Mechanical APDL and Mechanical Applications. Canonsburg, PA: Ansys Incorporation.

Ansys Inc. (2009b). Element Reference. Canonsburg, PA: Ansys Incorporation.

Desayi, P., & Krishnan, S. (1964). Equation for the Stress-Strain Curve of Concrete. ACI Journal, Volume 61, 345-350.

Hsu, C. T., Punurai, S., & Munoz, P. (2010). Patent No. 7,779,590. USA.

Majdi, Y. (2013). Finite Element Analysis of Composite Floors with Cold-formed Steel and Concrete Slab. Newark, NJ: NJIT, PhD Dissertation.

Punurai, S. (2007). Behavior of Composite Beams with Cold-Formed Steel Joists and Concrete. Newark, NJ: NJIT, PhD Dissertation.